第48卷第1期
2008年1月

大 连 理 工 大 学 学 报
Journal of Dalian University of Technology

Vol. 48, No. 1
Jan. 2008

化学化工、动力工程

文章编号：1000-8608(2008)01-0012-06

Growth kinetics and morphological structure of porous anodic aluminum oxide films formed in oxalic acid

MA Di*, LI Shu-ying

(School of Chem. Eng., Dalian Univ. of Technol., Dalian 116012, China)

Abstract: The growth kinetics of porous anodic aluminum oxide films formed in 0.3 mol · L^{-1} oxalic acid under galvanostatic conditions were studied to analyze the relationship between the anodizing conditions and the film morphology parameters. The effects of anodizing conditions (i.e. current density, temperature and anodizing time) on the film growth kinetics and morphology were examined by scanning electron microscopy and oxide film mass measurements. The electrochemical signatures were investigated by the voltage-time transients, and the growth rate of the anodic oxide films was predicted by the simple linear regression analysis. Experimental results indicate that the film growth rate increases with the increase of current density and the decrease of the temperature. The rate of increase of the film mass increases with an increase of current density.

Key words: anodic aluminum oxide film; oxalic acid; growth kinetics

0 Introduction

Anodic aluminum oxide (AAO) film with highly ordered pore arrangement, controllable pore diameter and well-characterized morphology[1] has been widely used as a template in fabrication of nanomaterials and nanostructures since the pioneering work of Masuda's group[2]. For example, metallic nanowires[3-5] and hollow nanotube arrays[6,7] were synthesized by controlled electrodeposition of a metal salt in an AAO template.

Major factors determining the structural parameters of the AAO film have been investigated[8-11]. At least five major factors influence the film morphology, which include the current/voltage relationship, electrolyte type, electrolyte temperature, concentration and time. The first four of these factors are interdependent and no one factor can change without adversely affecting another[8]. In addition, the mechanisms of the porous structure formation have also been reported in the literature[12-16]. However, the potential of AAO as a template for nanofabrication has not been fully exploited and the systematic analysis has not been made on how the anodizing parameters affect the film morphology.

Recently, Patermarakis, *et al*[17,18] and Shawaqfeh, *et al*[19] have investigated the growth kinetics of AAO films formed in sulfuric and phosphoric acid, respectively. Oxalic acid has been selected by various research groups to widely fabricate AAO template. However, no studies have been reported on the growth kinetics of AAO film formed in oxalic acid.

Received by: 2006-11-10; **Revised by**: 2007-12-05.
Corresponding author: MA Di* (1975-), Female, Doc., E-mail: madi_2004@163.com.

In the present study, oxalic acid is chosen as the anodizing electrolyte and the anodization is carried out under galvanostatic and stirred conditions at different temperatures. The electrochemical signatures are observed using voltage-time transients during anodization. The film thickness and mass variation with time under various anodizing conditions are discussed.

1 Experimental

1.1 Sample preparation

An aluminum metal sheet with the purity of 99.35% and the thickness of 0.25 mm was used as the starting material. Prior to anodizing, the samples were ultrasonically degreased in ethanol for 3 min. Then specimens were thoroughly rinsed with deionized water and immersed in 1.5 mol·L^{-1} sodium hydroxide at 60 ℃ for 30 s to remove the natural oxide, immediately neutralized in 1.5 mol·L^{-1} nitric acid for 15 s, carefully rinsed with deionized water and air-dried.

1.2 Measurements

Anodizing was performed under galvanostatic conditions in 0.3 mol·L^{-1} oxalic acid solutions at current densities 5-20 mA·cm^{-2} and bath temperature 10-25 ℃. Two stainless steel plates with the same dimensions were used as cathode materials and the pretreated aluminum sheet was used as the anode in the electrochemical cell. The solution was stirred vigorously using a mechanical stirrer in order to accelerate the diffusion of the heat which was derived from the sample. After anodizing, the mass of oxide films was estimated by measuring the mass of the anodized sample before and after anodic oxide removal in a phosphochromic acid[11] (20 g pure chromic acid powder and 35 mL 85% phosphoric acid mixed with deionized water to make 1 L) at a temperature of 90 ℃.

The oxide formation was carried out for the required time under carefully controlled known conditions, and the sample was weighed: mass m_1. The general procedure in the oxide removal stage was to immerse the sample in the phosphochromic acid and reweigh it until a constant final sample mass was obtained. Following oxide removal, the sample was reweighed: mass m_2. Thus the oxide mass can be calculated directly by the relationship, which is shown as the following equation:

$$m = m_1 - m_2 \tag{1}$$

The thickness and pore morphology of the anodized samples were examined using a scanning electron microscope (SEM, KYKY-2800B and JSM-5600LV).

2 Results and discussion

2.1 Voltage-time transients

The effects of current density and temperature on voltage-time transients in 0.3 mol·L^{-1} oxalic acid are shown in Fig. 1. The measured voltage variation with time provides a qualitative measure of the electrochemical kinetic phenomena associated with the formation of porous AAO films.

The voltage initially increases linearly with time to a maximum value followed by a decline to a steady state value which is the same as the general three stages of anodization[15]. At the beginning of anodization, the dramatic increase in voltage accompanies the initial growth of the barrier layer. When the voltage reaches a maximum value, the barrier layer is formed. However, the film thickness is not uniform, which leads to some pores appearance in the thinner film fields. Then the film electric resistance decreases with the emergence of the pores, the voltage decreases subsequently[20]. After pores are formed, the continuous formation and dissolution of the barrier layer at the base of pores result in one dimensional displacement into the aluminum substrate. The dynamic balance between oxide formation and its dissolution is established by the requirement of constant electrical field across the barrier, thus the steady-state voltage is reached[21].

As shown in Fig. 1(a), an increase in current density resulted in an increase in the measured voltage at the state of porous oxide film formed,

which can be attributed to a gradual increase in the resistance to ion transport through the pores due to the fast continuous thickening of the porous film in oxalic acid. The decrease in ionic conductivity within the porous film and across the barrier layer caused an increase in the measured voltage.

As shown in Fig. 1(b), an increase in temperature resulted in a decrease in the measured voltage, which can be attributed to the effect of the temperature on the oxide dissolution rate at the base of the pores. This decrease in the voltage reflects the increase in temperature within the pores, which is due to the loss of convective heat transfer. This increase in the temperature is expected to enhance the chemical dissolution process along the pore walls leading to more oxide dissolution. Sufficient pore wall dissolution process especially close to the film surface may result in a decrease in the film thickness when the oxide between adjoining pores is dissolved.

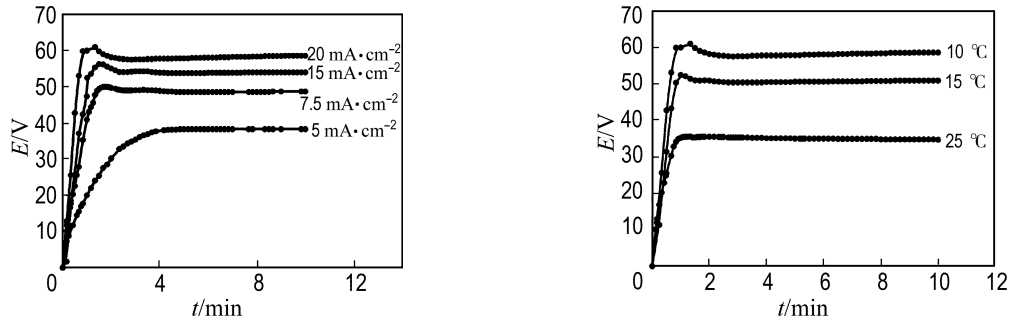

(a) different current densities (b) different temperatures

Fig. 1 The typical voltage-time behavior during galvanostatic anodizing of aluminum in 0.3 mol · L^{-1} oxalic acid

2.2 Film thickness and growth rate of AAO films

The film thickness was measured based on SEM images of cross sections of the AAO films. Fig. 2 shows representative SEM micrographs of the cross sections of anodic films formed in 0.3 mol · L^{-1} oxalic acid solution at 10 ℃ and 10 mA · cm^{-2} for different anodization time. The film thickness (h) variation with time at different current densities is shown in Fig. 3. It can be seen that the oxide film thickness increases linearly with time from zero, and finally reaches a maximum value.

The film growth rate, expressed as the film thickness increases per unit time, can be theoretically related to the Columbic efficiency of the anodic oxidation using Faraday's Law[22] as the following equation:

$$\frac{dh}{dt} = \eta \frac{M_{Al_2O_3}\, i}{\rho_0 z F} \tag{2}$$

Where dh/dt is the film growth rate, η is the current efficiency, $M_{Al_2O_3}$ is the molecular weight of the oxide, i is the current density, ρ_0 is the oxide density, z is the number of electrons used for oxide formation, and F is Faraday's constant.

This equation can be used for determining the film growth rate only if the current efficiency and the oxide density are known. Because of the uncertainties of two parameters, this equation can not be used to represent the actual film growth rate. According to Eq. (4), the film growth rate can be also expressed as the following equation:

$$dh/dt = k = k''i \tag{3}$$

Where k is the film growth rate and is a linear function of the current density, k'' is a constant. From the slope of the plots in Fig. 3, the film growth rate k is determined by simple linear regression analysis, as listed in Tab. 1, in which h is the mean thickness of the oxide film, t is the anodization time, and k'' is a constant independent of the current density and the anodization temperature. The film growth rate

increases from 1.411×10^{-6} $cm^3 \cdot mA^{-1} \cdot min^{-1}$ at 20 $mA \cdot cm^{-2}$ to 1.421×10^{-6} $cm^3 \cdot mA^{-1} \cdot min^{-1}$ at 10 $mA \cdot cm^{-2}$. By comparison, it is found that the increase in current density resulted in an increase in the film growth rate formed in oxalic acid, which can be attributed to the effect of current density on the rate of ion transport across the barrier layer.

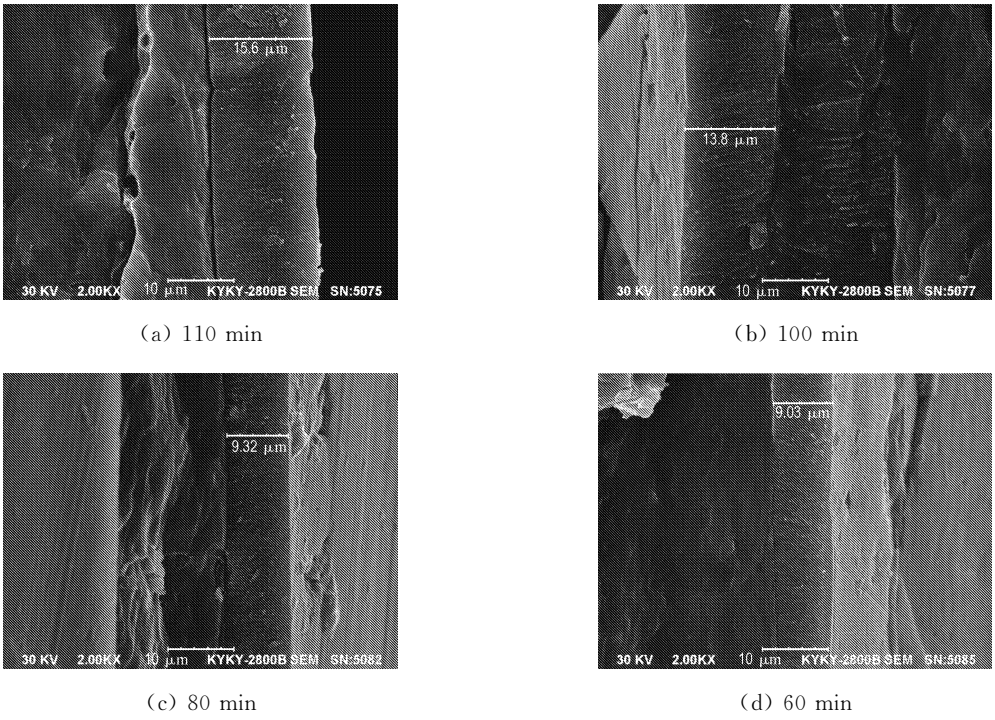

(a) 110 min　(b) 100 min

(c) 80 min　(d) 60 min

Fig. 2　SEM images of cross section of anodic film formed in 0.3 $mol \cdot L^{-1}$ oxalic acid solution at 10 ℃ and 10 $mA \cdot cm^{-2}$ for different anodization time

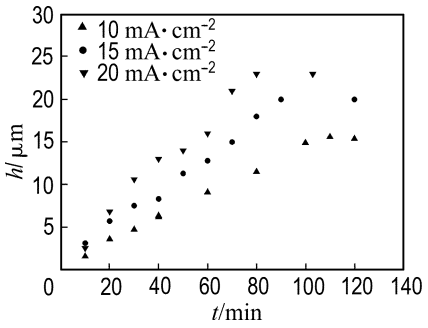

Fig. 3　Oxide film thickness as a function of the anodizing time at different current densities for films formed in 0.3 $mol \cdot L^{-1}$ oxalic acid solution at 10 ℃

Tab. 1　Regression equation of oxide film thickness at different current densities

i / $mA \cdot cm^{-2}$	Regression equations	k / $cm^3 \cdot mA^{-1} \cdot min^{-1}$	R^2
10	$h = 0.142\ 1t + 0.378$	1.421×10^{-6}	0.997
15	$h = 0.211\ 9t + 0.632$	1.413×10^{-6}	0.992
20	$h = 0.282\ 2t + 0.591$	1.411×10^{-6}	0.983

2.3　Effect of current density on the mass of oxide films

The dependence of the mass of the porous oxide film versus time on current density is shown in Fig. 4. At constant temperature and current density, the mass of the porous film was found to increase with time, which can be attributed to the growth of oxide film along the aluminum substrate based on the concept of the dynamic balance across the barrier layer. In addition, the rate of increase of film mass was found to increase with current density, which can be explained by the fact that the increase in the rate of transport of ions across the barrier layer leads to higher oxide formation rates. A similar trend was observed for the effect of current density on oxide thickness for film formed in oxalic acid.

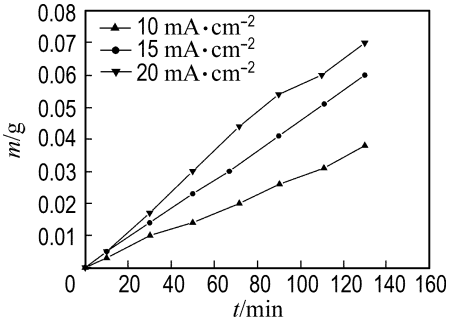

Fig. 4 Dependence of the oxide film mass on anodization time at different current densities for films formed in 0.3 mol·L^{-1} oxalic acid solution at 10 ℃

2.4 SEM measurement

SEM micrographs of the surface of anodic film before and after the dissolution of oxide are presented in Fig. 5. The hexagonally and uniformly ordered nanopores can be observed from Fig. 5(a), the pore diameters are about 135 nm with an average interpore center-to-center distance of about 214 nm, and a pore density of about 4×10^8 pores·cm^{-2}. Fig. 5(b) illustrates a perspective view of the aluminum substrate after dissolving the oxide film in phosphochromic acid at about 90 ℃. It is shown that the porous film has been totally removed and this aluminum substrate can be reused.

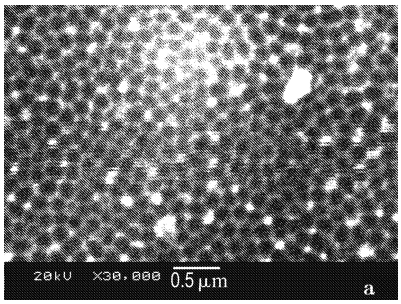

(a) surface of anodic film

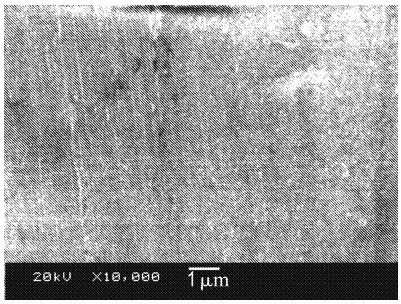

(b) aluminum substrate after dissolving the oxide film

Fig. 5 SEM images

3 Conclusions

The growth kinetics of porous anodic aluminum films formed in 0.3 mol·L^{-1} oxalic acid solutions was studied. The voltage-time transients show that the changing of current density and electrolyte temperature in oxalic acid influences the porous film growth. The thickness and the mass of the porous oxide films are found to depend on current density. In addition, the film growth can be expressed by the equation $dh/dt = k''i$, where k'' is a constant independent of the current density and the anodization temperature with an average value of 1.415×10^{-6} $cm^3\cdot mA^{-1}\cdot min^{-1}$.

References:

[1] KELLER F, HUNTER M, ROBINSON D. Structural features of oxide coatings on aluminum[J]. **J Electrochem Soc**, 1953, **100**(9): 411-419

[2] MASUDA H, FUKUDA K. Ordered metal nanohole arrays made by a two-step replication of honeycomb structures of anodic alumina [J]. **Science**, 1995, **268**(5216): 1466-1468

[3] DING J X, ZAPIEN J A, CHEN W W, *et al*. Lasing in ZnS nanowires grown on anodic aluminum oxide templates[J]. **Appl Phys Lett**, 2004, **85** (12): 2361-2363

[4] KHAN H R, PETRIKOWSKI K. Anisotropic structural and magnetic properties of arrays of $Fe_{26}Ni_{74}$ nanowires electrodeposited in the pores of anodic alumina [J]. **J Magn Magn Mater**, 2000, **215**: 526-528

[5] WHITNEY T M, JIANG J S, SEARSON P C, *et al*. Fabrication and magnetic properties of arrays of metallic nanowires [J]. **Science**, 1993, **261**(5126): 1316-1319

[6] CHEN P L, CHANG J K, KUO C T, *et al*. Field emission of carbon nanotubes on anodic aluminum oxide template with controlled tube density [J]. **Appl Phys Lett**, 2005, **86**(12): 1-3

[7] KOHLI P, WHARTON J E, BRAIDE O, *et al*. Template synthesis of gold nanotubes in an anodic alumina membrane [J]. **J Nanosci Nanotech**, 2004,

4(6): 605-610

[8] HUNTER M S, FOWLE P. Factors affecting the formation of anodic oxide coatings [J]. **J Electrochem Soc**, 1954, **101**(10): 514-516

[9] THOMPSON G E. Porous anodic alumina: fabrication, characterization and applications [J]. **Thin Solid Films**, 1997, **297**(1-2): 192-201

[10] THOMPSON G E, WOOD G C. Porous anodic film formation on aluminium [J]. **Nature**, 1981, **290**: 230-232

[11] YOUNG L. **Anodic Oxide Films** [M]. New York: Academic Press, 1961

[12] JESSENSKY O, MULLER F, GOSELE U. Self-organized formation of hexagonal pore structures in anodic alumina [J]. **J Electrochem Soc**, 1998, **145**(11): 3735-3740

[13] MASUDA H, YAMADA H, SATOH M, *et al*. Highly ordered nanochannel-array architecture in anodic alumina [J]. **Appl Phys Lett**, 1997, **71**(19): 2770-2772

[14] THOMPSON G E, FURNEAUX R C, WOOD G C, *et al*. Nucleation and growth of porous anodic films on aluminum[J]. **Nature**, 1978, **272**: 433-435

[15] O'SULLIVAN J P, WOOD G C. The morphology and mechanism of formation of porous anodic films on aluminium[J]. **Proc Roy Soc Lond A:Math and Phys Sci**, 1970, **317** (1531): 511-543

[16] PATERMARAKIS G, PAPANDREADIS N. Effect of the structure of porous anodic Al_2O_3 films on the mechanism of their hydration and pore closure during hydrothermal treatment [J]. **Electrochim Acta**, 1993, **38**(10): 1413-1420.

[17] PATERMARAKIS G, TZOUVELEKIS D. Development of a strict kinetic model for the growth of porous anodic Al_2O_3 films on aluminum[J]. **Electrochim Acta**, 1994, **39** (16): 2419-2429

[18] PATERMARAKIS G, PAPANDREADIS N. Study on the kinetics of growth of porous anodic Al_2O_3 films on Al metal [J]. **Electrochim Acta**, 1993, **38**(15): 2351-2361

[19] SHAWAQFEH A T,BALTUS R E. Growth kinetics and morphology of porous anodic alumina films formed using phosphoric acid [J]. **J Electrochem Soc**, 1998, **145**(8): 2699-2706

[20] DIGGLE J W, DOWNIE T C,GOULDING C W. Anodic oxide films on aluminum [J]. **Chem Rev**, 1969, **69**: 365-405

[21] PARKHUTIK V P, ALBELLA J M, MAKUSHOK Y E, *et al*. Study of aluminium anodization in sulphuric and chromic acid solutions. I. Kinetics of growth and composition of oxides [J]. **Electrochim Acta**, 1990, **35**(6): 955-960

[22] HEBER K V. Studies on porous Al_2O_3 growth. Pt. 2. Ionic conduction [J]. **Electrochim Acta**, 1978, **23**(2): 135-139

草酸中多孔阳极氧化铝膜生长动力学和形态结构研究

马　迪*，李淑英

（大连理工大学 化工学院，辽宁 大连　116012）

摘要： 为分析多孔阳极氧化铝膜形态参数和氧化条件的关系，在恒流条件下对 0.3 mol·L^{-1}草酸电解中形成多孔膜的生长动力学进行了研究. 采用扫描电子显微镜和氧化膜质量测定方法检验了电流密度、温度和氧化时间对氧化膜生长动力学和氧化膜形态的影响. 通过电压-时间曲线研究了氧化膜的电化学特征，并采用一元线性回归模型预测了氧化膜的生长速率. 实验结果表明氧化膜的生长速率随电流密度的升高而升高，随温度的升高而下降. 氧化膜质量的增长速率也随着电流密度的升高而增大.

关键词： 阳极氧化铝膜；草酸；生长动力学

中图分类号： TQ153.6　　**文献标志码：** A

收稿日期： 2006-11-10；　**修回日期：** 2007-12-05.

作者简介： 马　迪*(1975-)，女，博士生，E-mail:madi_2004@163.com.